UNIVERSITA' DEGLI STUDI DI BERGAMO
DIPARTIMENTO DI INGEGNERIA GESTIONALE E DELL'INFORMAZIONE[°]
QUADERNI DEL DIPARTIMENTO[†]

Department of Management and Information Technology

Working Paper

Series "*Mathematics and Statistics*"

n. 14/MS – 2006

Analytical procedures to study general cross section wires during nonlinear bending

by

Sergio Baragetti, Giacomo Gigante and Federico Tordini

[°] Viale Marconi. 5, I – 24044 Dalmine (BG), ITALY, Tel. +39-035-2052339; Fax. +39-035-562779
[†] Il Dipartimento ottempera agli obblighi previsti dall'art. 1 del D.L.L. 31.8.1945, n. 660 e successive modificazioni.

[§] L'accesso alle *Series* è approvato dal Comitato di Redazione. I *Working Papers* ed i *Technical Reports* della Collana dei Quaderni del Dipartimento di Ingegneria Gestionale e dell'Informazione costituiscono un servizio atto a fornire la tempestiva divulgazione dei risultati dell'attività di ricerca, siano essi in forma provvisoria o definitiva.

Analytical procedures to study general cross section wires during nonlinear bending

Sergio Baragetti[a], Giacomo Gigante[b], Federico Tordini[c]

[a] *Dipartimento di Progettazione e Tecnologie, Università degli Studi di Bergamo, Viale Marconi 5 - 24044 Dalmine, Italy. E-mail: sergio.baragetti@unibg.it.*

[b] *Dipartimento di Ingegneria Gestionale e dell'Informazione, Università degli Studi di Bergamo, Viale Marconi 5 - 24044 Dalmine, Italy. E-mail: giacomo.gigante@unibg.it.*

[c] *Dipartimento di Ingegneria, Università degli Studi di Ferrara, Via Saragat 1 - 44100 Ferrara, Italy. E-mail: federico.tordini@unibg.it.*

ABSTRACT

Nonlinear bending of thin wires is the main or one of the fundamental matters in several applications, especially when the plastic behaviour is widely involved. Such applications often require the reaching of large curvatures if compared to wire cross-section dimensions. In these cases a broad plasticization of the cross section is achieved early, even before curvature becomes large. In this paper a new analytical model is proposed, able to foresee the final curvature obtained after nonlinear bending of wires with non-symmetric cross sections, once load parameters are known. Both elastic springback after the unloading and material behavioural nonlinearities have been considered. From the engineering point of view, negligible errors are committed when applying the model to all those materials guaranteeing that wire cross sections remain plane after rotation (Bernoulli-Navier's hypothesis). The wire stress state can be evaluated by means of the model and enables the low cycle fatigue resistance verification.

Keywords: Thin wires, bending, large curvature, analytical model, low cycle fatigue.

1. INTRODUCTION

For those structural applications involving thin wire bending that require the achievement of small residual final curvature radii, even comparable to the dimensions of the cross section, a good knowledge of the bending process technological parameters is essential. The designer would be greatly helped by a reference calculation model that could assess them. Among the most common examples of applications that can benefit by the utilization of a specific model, recall the production of bent wires for tyre, cylindrical helical spring or spectacle frame manufacturing. The metallic materials manageable by means of the model should also be different from classical carbon steel, *e.g.* titanium or aluminium alloys. Moreover, the maximum wire stress and strain state during bending should be estimable by applying the model in order to avoid excessive wire damaging or fatigue failure. Further greatly developing applications, like those utilizing shape memory bent wires constructed with particular Ti-Ni alloys [1-3], *e.g.* the production of orthodontic wires [4-6], can be interested in such a model.

The very accurate analytical methods dealing with the nonlinear bending of plates, that can be found in the literature [7-9], are not applicable to wires because of the substantial geometric differences between the two technological products. For example, assuming the hypothesis of compact cross section about its centroid, a plate shows the anticlastic effect. The models in the literature enable to determine with high accuracy the technological parameters necessary to obtain the required final shapes for metal plates, taking into account the elastic springback after folding operations [10]. J.F. Wang *et al.* [11] proposed an in-depth study on the folding of aluminium alloy sheets taking into account the effect of the anticlastic curvature on the elastic springback. The authors pointed out the effect of the plate geometrical parameter variation on the zone of persistent anticlastic curvature and on the final shape of the manufactured product. Other models [12] studied the correlation between the bending process and the mechanical characteristics of materials. The development and diffusion of the Finite Element method has allowed to improve and realize several calculation models based on the numerical simulation of bending processes. Such studies allow to estimate with accuracy the springback of the metallic sheets after unloading during folding operations so as to provide the designer with a quick and precise tool that optimizes process technological parameters [13-19]. B.K. Chun *et al.* [20, 21] studied and implemented models by means of finite elements, able to simulate sheet metal forming operations taking into account the Bauschinger's effect, and to foresee the elastic springback in presence of cyclic load. The material work hardening was considered by means of nonlinear isotropic and kinematic behavioural models. In the literature, further analytical and numerical-iterative models are available. They allow to foresee the plate elastic springback and to optimize sheet folding and forming operations and die

design [22-25]. All these models have also been validated by the comparison with experimental data.

As aforesaid, research studies of nonlinear bending of metallic wires have not known, for the time being, the same development that has interested the studies of sheet metal folding and forming. Studies [26-28] reported in less recent literature are focused on the calculation of the bending angle recovered by means of elastic springback by rectangular cross sectioned wires after a uniform bending process with known radius of curvature. The results obtained by applying the analytical model reproduce accurately the experimental evidences if the residual stress effect on the wire is left aside. I.V. Khromov [29] elaborated a calculation algorithm and implemented, starting from it, a FEM model for determining the stress state of effort in a wire with circular cross section. The numerical solution of the problem was obtained using integral equations valid in the plasticized zone of the cross section and considering a material with linear isotropic work hardening behaviours. B. Goes *et al.* [30] formulated an analytical model to describe the effect of the residual stresses on tensile tests after coiling or bending operations. The coiling curvature is large if compared to the wire cross section radius and it is assumed that the material behaviour fits the Voce law, and the Bauschinger's effect on the elastic springback is negligible. Residual stresses and a highly work hardened material are effects of the wire drawing process. C.J. Luis *et al.* [31] proposed a comparison between analytical and numerical methods applied to the study of wire drawing. S.H. Chen and T.C. Wang [32] studied the bending of thin beams experimentally, in order to formulate a new work hardening law of the strain gradient theory. In the reference, elastic springback after unloading and the following residual curvature are not dealt with. J.Y. Richard Liew *et al.* [33] analyzed curved beams to evaluate, taking into account the residual stresses and the radius of curvature, the ultimate moment capacity by means of an analytical model and with the aid of a finite element model. In the literature, one can find references on the nonlinear bending of curved beams in plain strain state, considering the material work hardening [34]. Other references report studies on beams bending in presence of a residual stress field [35], and on the nonlinear bending of sandwich beams by means of analytical and experimental methods [36].

The aim of this paper is to develop, starting from the model proposed in the reference [37], a more accurate analytical model able to improve the models available in the literature in foreseeing the residual curvature produced in thin metallic wires after bending operations. Thanks to the determination of the stress state over the wire cross section, it also enables to analyze the low cycle fatigue resistance during service life. The calculation model could supply a designer with an accurate and, at the same time, simple and fast tool to deduce *a priori* the required bending moment or the loading radius of curvature. In order to do it, the model takes into account the nonlinear

material behaviour during bending, *i.e.* it can consider either the whole cross section in the elastic field or partially elastic and partially plastic or entirely in the plastic field. The curvature loss during unloading elastic springback or the material post-yielding plasticization are therefore not neglected. The bending process nonlinearity, that the model takes into account, has a high influence on the accuracy of the imposed design process curvature, in particular when large curvatures, *i.e.* large deformations, are involved. One of the main aspects of the work is the study of the neutral axis displacement for a generic cross section, when the reached curvature determines the beginning of the wire plasticization [38]. The model takes into account this effect, even if it does not appear explicitly in any calculation step. Moreover, the final strain level for a bent wire can be accurately predicted so as to avoid obtaining excessively damaged or failed final products. Among all the material behaviour laws proposed in the literature [39-44] for modeling the correlation between stress and deformation, we have chosen the elastic-perfectly plastic material behaviour. In future developments, we intend to verify the possibility to extend the model validity to other and more accurate material behaviour models.

The cross section geometries that can be studied by the model are generic. In the present work, the study of a singly symmetric cross section similar to those of spectacle frames has been developed in full detail. We assume, among our starting theoretical hypotheses, the Bernoulli-Navier's hypothesis about the conservation of the cross section planarity after rotations, and the hypothesis of compact cross section around the centroid so as to be able to neglect deformation anticlastic effects. At the end of the paper, a numerical example of model application on a wire with singly symmetric cross section is implemented with the aid of a suitable calculation code. The example also shows the displacements of the neutral axis and of the advancing plasticization fronts over the cross section with the diminishing of the radius of curvature during the process progression.

2. ANALYTICAL MODEL: HYPOTHESES AND DEVELOPMENT

First of all we point out some fundamental statements and preliminary hypotheses:

1) The starting wire configuration is rectilinear and then the bending follows an arc of circumference whose radius decreases during the loading phase. We call r the actual radius of curvature due to the bending load with respect to the cross section centroidal axis. The starting wire bendable length has been called l_0.
2) We suppose that wire cross sections remain plane after bending rotation and oriented as the radial direction from the centre of curvature (Bernoulli-Navier's hypothesis). From point 1) the curvature is the same for all the sections belonging to l_0.

3) We neglect transversal and shear stresses during bending with respect to normal ones.
4) We fix each cross section *y* vertical axis directed towards the centre of curvature. The *y* axis origin is kept fixed on cross section centroid during bending and let positive *y* values be on the centre of curvature side.
5) Let $b(y)$ be the wire cross section width varying with the *y* coordinate so that the cross section area is:

$$A = \int_{-\infty}^{\infty} b(y)\, dy \tag{1}$$

Clearly $b(y)$ is null outside the cross section height interval.
6) By the hypothesis 4) on the centroid, the following equation has to be satisfied:

$$\int_{-\infty}^{\infty} b(y)\, y\, dy = 0 \tag{2}$$

7) In order to determine the actual wire configuration during nonlinear bending with respect to the actual curvature radius, it is necessary to evaluate, by means of the equilibrium equation, the actual $y = y(r)$ curvature angle spanned by the wire (figure 1).
8) The engineering strain of a generic fibre positioned at the *y* quote is therefore given by:

$$e_e(r, y) = \frac{y\,(r)(r-y) - l_0}{l_0} = \frac{y\,(r)(r-y)}{l_0} - 1 \tag{3}$$

9) In the pure elastic field of material behaviour the actual strain can be assumed substantially equal to the engineering one. In the plastic field the true strain formulation has instead to be applied. This distinction is not important for the calculation procedure here reported but only for the final check about the not overcoming of the material plastic strain limit (rupture). In fact the model equations do not involve integrations with respect to strains but to *y* cross section quotes. In symbols:

$$\begin{cases} e(r,y) = e_e(r,y) & \text{if} \quad e \le e_s \\ e(r,y) = ln\left(1 + e_e(r,y)\right) & \text{if} \quad e \ge e_s \end{cases} \tag{4}$$

It is important to emphasize that the model proposed in this paper applies only if the real material behaviour can guarantee a substantial respect of Bernoulli-Navier's hypothesis for cross section rotations during nonlinear bending. From the engineering point of view it could be said that most technical application materials are treatable considering point 2) satisfied with negligible discrepancies.

In the present model, an elastic-perfectly plastic material behaviour is considered, with symmetric

tension and compression behaviours. For next research activities, more complicated and realistic behavioural models will be evaluated, even if we judge the results reached considering this simple first model quite satisfying and opening to further study developments.

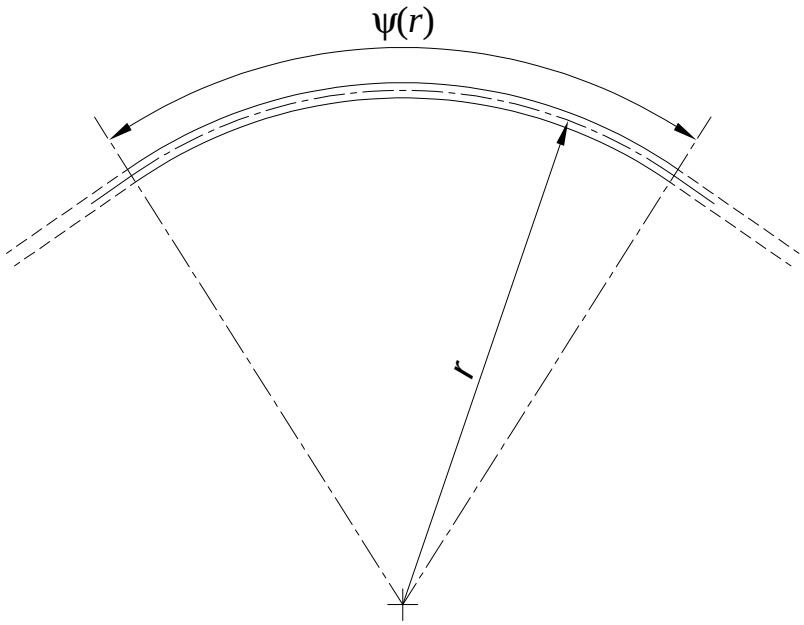

Figure 1: actual curvature angle representation.

2.1 Perfectly elastic range

In the pure elastic range of the material behaviour the normal stress in a generic cross section point with vertical coordinate *y* is given by:

$$s\,(r, y) = E\,e\,(r, y) \quad \text{if} \quad \left|e\,(r, y)\right| \le e_s \tag{5}$$

Assuming that the applied bending moment is uniform along the bent wire, the equilibrium equation for a generic cross section is:

$$\int_{-\infty}^{\infty} s\,(r,\, y)\, b(y)\, dy = 0 \qquad \forall r \tag{6}$$

Substituting the stress expression from equation (5) we obtain:

$$0 = E \int_{-\infty}^{\infty} \left[\frac{y\,(r)(r-y)}{l_0} - 1 \right] b(y)\, dy$$

$$\Leftrightarrow \int_{-\infty}^{\infty} \frac{y\,(r)(r-y)}{l_0} b(y)\, dy - \int_{-\infty}^{\infty} b(y)\, dy = \frac{y\,(r)}{l_0} \int_{-\infty}^{\infty} (r-y)\, b(y)\, dy - A = 0 \tag{7}$$

The analytical formulation for $y(r)$ is thus obtained:

$$y\,(r)=\frac{A}{\int_{-\infty}^{\infty}\frac{r-y}{l_0}b(y)\,dy}=\frac{Al_0}{r\int_{-\infty}^{\infty}b(y)\,dy-\int_{-\infty}^{\infty}yb(y)\,dy}=\frac{Al_0}{rA}=\frac{l_0}{r} \tag{8}$$

In this case the actual strain expression is reduced to:

$$e\,(r,\,y)=\frac{\frac{l_0}{r}(r-y)-l_0}{l_0}=-\frac{y}{r} \tag{8}$$

The wire length at a generic *y* quote for each actual curvature radius is:

$$l(r,\,y)=y\,(r)(r-y) \tag{9}$$

By equating the partial derivative of *l* with respect to *r* with zero we are able to verify that, as expected for the pure elastic field, the cross section centroid lies on the neutral axis:

$$\frac{\partial l}{\partial r}(r,\,y)=\frac{\partial}{\partial r}\left[\frac{l_0}{r}(r-y)\right]=0\;\Leftrightarrow\;\frac{l_0 y}{r^2}=0 \tag{10}$$

This represents a first check for the analytical model correctness. The applied bending moment during the wire loading phase can be calculated as follows:

$$M(r)=\int_{-\infty}^{\infty}s\,(r,y)(y-y_n)b(y)\,dy=E\int_{-\infty}^{\infty}e\,(r,y)yb(y)\,dy=\frac{-E}{r}\int_{-\infty}^{\infty}y^2b(y)\,dy=-\frac{EJ_C}{r} \tag{11}$$

In this case the springback after unloading is theoretically complete so that no residual curvature can be observed. Obviously this behaviour involves only large curvature radii. As the curvature rises and the elastic limit is exceeded, the influence of the plastic field behaviour has to be adequately considered.

2.2 Perfectly elastic-perfectly plastic range

Since an elastic-perfectly plastic material behaviour is assumed, as the yield stress is achieved further deformations do not generate any increase in the stress level. Consequently in the perfectly plastic field the stress can be expressed as follows:

$$s\,(r,\,y)=\begin{cases}Ee_s & \text{if } e\,(r,\,y)>e_s\\ -Ee_s & \text{if } e\,(r,\,y)<-e_s\end{cases} \tag{12}$$

It has to be pointed out that as the first fibre of the cross section begins to yield, the neutral axis position begins to move in order to guarantee the undeformed condition for the neutral fibre. The unloading of the wire can not restore the undeformed state for the plasticized fibres anymore as is for the pure elastic range. A residual curvature begins to be observed.

Let $y_1(r)$ be the quote at which the first yielding in the outer side with respect to the centre of curvature happens, and $y_2(r)$ for the inner one, without considering if each quote is or is not inside the cross section height limits. In order to determine y_1 and y_2 for a given radius of curvature r, it has to be understood which fibres have already been yielded and which not over the cross section. The non-plasticized fibres are included in the following interval:

$$\left|e\left(r,\, y\right)\right| = \left|\frac{y\,(r)(r-y)}{l_0} - 1\right| \le e_s \quad \Leftrightarrow \quad y_1 = r - \frac{(1+e_s)l_0}{y\,(r)} \le y \le r - \frac{(1-e_s)l_0}{y\,(r)} = y_2 \tag{13}$$

By linearity, the neutral axis quote is centred in the above reported elastic interval, thus:

$$y_n\left(r\right) = r - \frac{l_0}{y\,(r)} \tag{14}$$

Rearranging the adopted material behaviour in terms of y, the normal stress over the cross section can be reformulated as follows:

$$s\,(r,\, y) = \begin{cases} Ee_s & \text{if} \quad y \le r - \frac{(1+e_s)l_0}{y\,(r)} \\ E\left(\frac{(r-y)y\,(r)}{l_0} - 1\right) & \text{if} \quad r - \frac{(1+e_s)l_0}{y\,(r)} \le y \le r - \frac{(1-e_s)l_0}{y\,(r)} \\ -Ee_s & \text{if} \quad r - \frac{(1-e_s)l_0}{y\,(r)} \le y \end{cases} \tag{15}$$

The curvature angle is obtained from the equilibrium equation as for equation (6). In this case the integral formulation is more complicated:

$$\int_{-\infty}^{\infty} s\,(r,\, y)\, b(y)\, dy = 0$$

$$e_s \int_{-\infty}^{r - \frac{(1+e_s)l_0}{y\,(r)}} b(y)\, dy + \int_{r - \frac{(1+e_s)l_0}{y\,(r)}}^{r - \frac{(1-e_s)l_0}{y\,(r)}} \left[\frac{y\,(r)(r-y)}{l_0} - 1\right] b(y)\, dy - e_s \int_{r - \frac{(1-e_s)l_0}{y\,(r)}}^{\infty} b(y)\, dy = 0 \tag{16}$$

Note here that formulation (15) holds if and only if y_1 and y_2 are respectively decreasing and increasing as functions of the curvature radius r. Otherwise one would have the paradoxical situation where an already plasticized fibre returns to an elastic behaviour. Observe that:

$$\frac{\partial y_1}{\partial r} = \frac{1+e_s}{y^{\,2}} l_0 \frac{dy}{dr} + 1 \tag{17}$$

and, by an application of the implicit function theorem:

$$\frac{dy}{dr} = -\frac{y\int_{y_1}^{y_2} b(y)\,dy}{\int_{y_1}^{y_2}(r-y)b(y)\,dy} \tag{18}$$

Therefore, substituting (18) in (17), one obtains:

$$\frac{\partial y_1}{\partial r} = \frac{\int_{y_1}^{y_2}(y_1-y)b(y)\,dy}{\int_{y_1}^{y_2}(r-y)b(y)\,dy} < 0 \tag{19}$$

and this shows that y_1 decreases with r. Similarly, one can prove that:

$$\frac{\partial y_2}{\partial r} = \frac{\int_{y_1}^{y_2}(y_2-y)b(y)\,dy}{\int_{y_1}^{y_2}(r-y)b(y)\,dy} > 0 \tag{20}$$

and y_2 indeed increases with r.

By developing equation (16) it is possible to calculate $y(r)$ as an explicit function of the radius of curvature and by means of its value the applied bending moment:

$$M(r) = \int_{-\infty}^{\infty} s\,(r,y)(y-y_n)b(y)\,dy = \int_{-\infty}^{\infty} s\,(r,y)\,yb(y)\,dy$$

$$\begin{aligned} M(r) = {} & Ee_s\int_{-\infty}^{r-\frac{(1+e_s)l_0}{y(r)}} b(y)\,y\,dy + E\int_{r-\frac{(1+e_s)l_0}{y(r)}}^{r-\frac{(1-e_s)l_0}{y(r)}}\left[\frac{y(r)(r-y)}{l_0}-1\right]b(y)\,y\,dy + \\ & -Ee_s\int_{r-\frac{(1-e_s)l_0}{y(r)}}^{\infty} b(y)\,y\,dy \end{aligned} \tag{21}$$

It is simple to analytically determine the neutral axis position corresponding to the fully plasticized cross section, provided that such condition be reached. In this case the equilibrium equation becomes, as well-known from the classical Structural Mechanics literature:

$$e_s\int_{-\infty}^{y_n} b(y)\,dy - e_s\int_{y_n}^{\infty} b(y)\,dy = 0 \quad\Leftrightarrow\quad \int_{-\infty}^{y_n} b(y)\,dy = \int_{y_n}^{\infty} b(y)\,dy \tag{22}$$

It is trivial to understand that the neutral axis divides the cross section into two fully plasticized parts of the same area.

The model above reported is applicable to a generic wire cross section. The rising complications introduced when we try to apply the model to a precise cross section shape are not irrelevant. In the following part of the paper the case of a singly symmetric cross section will be treated.

As a final remark of this section, observe that, when applied to a doubly symmetric cross section wire ($b(y) = b(-y)$), this model recovers the results obtained by S. Baragetti [37] in the case of

elastic-perfectly plastic material behaviour. Indeed the equilibrium equation is verified by the function $y(r) = l_0/r$ for any value of r:

$$e_s\int_{-\infty}^{r-\frac{(1+e_s)l_0}{l_0/r}} b(y)\,dy+\int_{r-\frac{(1+e_s)l_0}{l_0/r}}^{r-\frac{(1-e_s)l_0}{l_0/r}}\left[\frac{l_0}{r}\frac{(r-y)}{l_0}-1\right]b(y)\,dy-e_s\int_{r-\frac{(1-e_s)l_0}{l_0/r}}^{\infty} b(y)\,dy=0$$

$$\Leftrightarrow\quad e_s\int_{-\infty}^{-e_s r} b(y)\,dy-\frac{1}{r}\int_{-e_s r}^{e_s r} yb(y)\,dy-e_s\int_{e_s r}^{\infty} b(y)\,dy=0 \tag{23}$$

The angle $y(r)$ spanned by the bent wire arc is the same already found for the perfectly elastic behaviour range. The neutral axis remains coincident with the centroidal axis until fully plasticization of the cross section is achieved.

Substituting the expression for y into equation (21) one can easily obtain the bending moment:

$$\begin{aligned} M(r) &= Ee_s\int_{-\infty}^{-e_s r} b(y)\,y\,dy-\frac{E}{r}\int_{-e_s r}^{e_s r} b(y)\,y^2\,dy-Ee_s\int_{e_s r}^{\infty} b(y)\,y\,dy= \\ &= -2Ee_s\int_{e_s r}^{\infty} b(y)\,y\,dy-\frac{2E}{r}\int_{0}^{e_s r} b(y)\,y^2\,dy \end{aligned} \tag{24}$$

3. SINGLY SYMMETRIC CROSS SECTION

Starting from the model discussed in the previous section, we have developed the study of nonlinear bending of a singly symmetric cross section wire. It has to be noted the relevance of this section shape because of its large diffusion, *e.g.* in the spectacle frame field. In figure 2 the studied cross section shape is represented. The concavity realized in the section bottom side could in particular receive the lens external edge and keep it fixed.

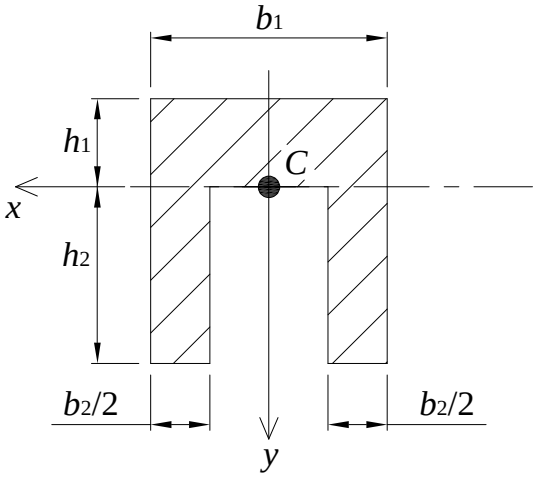

Figure 2: the singly symmetric cross section type considered in the model.

The centroid lies on the width changing quote and the symmetry axis coincides with the vertical y axis and crosses C. With respect to the coordinate system we have:

$$b(y)=\begin{cases} b_1 & \text{if} \quad -h_1 \le y \le 0 \\ b_2 & \text{if} \quad 0 \le y \le h_2 \end{cases} \tag{25}$$

Provided that $h_1 < h_2$, from the application of equation (2) results:

$$\int_{-h_1}^{h_2} b(y)\, y\, dy = 0 \quad \Leftrightarrow \quad b_1 h_1^2 = b_2 h_2^2 \tag{26}$$

Let d be the ratio $h_2/h_1 > 1$, then it is useful to express b_1 and h_1 as functions, respectively, of b_2 and h_2:

$$\begin{cases} b_1 = d^{\,2} b_2 \\ h_1 = d^{-1} h_2 \end{cases} \tag{27}$$

The area of the cross section part where the y coordinates are negative is bigger than the one where they are positive. Indeed $b_1 h_1 = d\, b_2 h_2 > b_2 h_2$. As a consequence, for the fully plasticized wire cross section, the neutral axis quote y_n has to be negative in order to verify the condition of the equality between inner and outer area (22). In symbols we have:

$$(y_n + h_1) b_1 = b_2 h_2 - y_n b_1 \quad \Leftrightarrow \quad y_n = -\frac{b_1 h_1 - b_2 h_2}{2 b_1} = -\frac{d-1}{2d} h_1 \tag{28}$$

This coordinate varies from 0 to $-h_1/2$ with d varying from 1 to infinity.
It is easy to evaluate the bending moment that plasticizes the whole cross section:

$$M_{fp} = \int_{-h_1}^{y_n} s_s b_1\, y\, dy - \int_{y_n}^{0} s_s b_1\, y\, dy - \int_{0}^{h_2} s_s b_2\, y\, dy = \frac{E e_s b_1}{2}\left(y_n^2 - h_1^2\right) + \frac{E e_s b_1}{2} y_n^2 - \frac{E e_s b_2}{2} h_2^2$$

$$\Rightarrow M_{fp} = -\frac{E e_s}{4 d^2}(3d-1)(d+1) b_2 h_2^2 \tag{29}$$

Now we are able to formulate a hypothesis about the y_1 and y_2 limit trend of the non-plasticized intermediate region of the cross section with the variation of r. In particular, given that for small curvature we have an elastic behaviour, while for full plasticization the neutral axis has negative coordinate, we can identify only two different possible trends.
For the first one we can select three particular curvature radius values, r_1, r_2 and r_3, with $r_3 < r_2 < r_1$, such that four cases are observable:

$$y_1 \le -h_1 \le 0 \le h_2 \le y_2 \quad \text{if} \quad r_1 \le r \tag{30-a}$$

$$y_1 \le -h_1 \le 0 \le y_2 \le h_2 \quad \text{if} \quad r_2 \le r \le r_1 \tag{30-b}$$

$$-h_1 \le y_1 \le 0 \le y_2 \le h_2 \quad \text{if} \quad r_3 \le r \le r_2 \tag{30-c}$$

$$-h_1 \le y_1 \le y_2 \le 0 \le h_2 \quad \text{if} \quad r \le r_3 \tag{30-d}$$

In figure 3 the third case of (30) is represented as an example.

For the second possibility we can suppose that the three values make true the following set of situations:

$$y_1 \le -h_1 \le 0 \le h_2 \le y_2 \quad \text{if} \quad r_1 \le r \tag{31-a}$$

$$y_1 \le -h_1 \le 0 \le y_2 \le h_2 \quad \text{if} \quad r_2 \le r \le r_1 \tag{31-b}$$

$$y_1 \le -h_1 \le y_2 \le 0 \le h_2 \quad \text{if} \quad r_3 \le r \le r_2 \tag{31-c}$$

$$-h_1 \le y_1 \le y_2 \le 0 \le h_2 \quad \text{if} \quad r \le r_3 \tag{31-d}$$

From (31) one can argue that the plasticization of the centroidal fibre happens before that of the $-h_1$ quoted fibre. But this can not happen because for $r = r_3$, namely while the $-h_1$ quoted fibre is plasticizing, the equilibrium equation would not be satisfied:

$$\int_{-h_1}^{y_2} \left[\frac{(r_3 - y)y}{l_0} - 1 \right] b_1 \, dy - e_s \int_{y_2}^{0} b_1 \, dy - e_s \int_{0}^{h_2} b_2 \, dy = 0$$

$$\Leftrightarrow \quad b_1 \int_{-h_1}^{y_2} \left[\frac{(r_3 - y)y}{l_0} - 1 \right] dy = -e_s b_1 y_2 + e_s h_2 b_2$$

In fact for the elastic region of the cross section we have:

$$\int_{-h_1}^{y_2} \left[\frac{(r_3 - y)y}{l_0} - 1 \right] dy = 0$$

So we get the following absurd (recalling that $y_2 \le 0$):

$$0 = -e_s y_2 b_1 + e_s h_2 b_2 > 0 \tag{32}$$

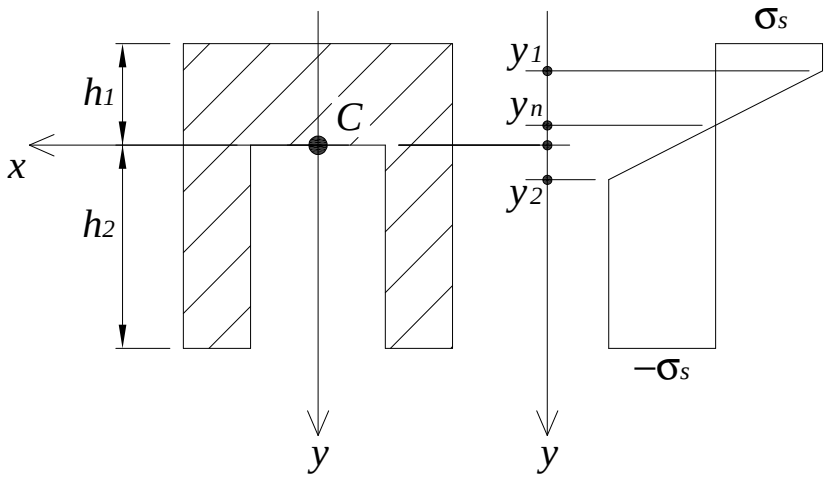

Figure 3: example of a possible stress state during bending. In particular the c-case is showed.

Then the cases collected in (31) have to be discarded. Applying the cases (30-a), (30-b), (30-c) or (30-d) the equilibrium equation (16) changes when applied to each one of them. The result that we have obtained is a piecewise smooth function $y(r)$ covering all the range of curvature radii up to the smallest ones. Clearly the choice of the correct solutions for each radius interval is dependent on the continuity condition at its extremes.

For the case (30-a), when the cross section is fully perfectly elastic, the equilibrium equation (16) reduces to:

$$\int_{-h_1}^{h_2}\left[\frac{(r-y)y'(r)}{l_0}-1\right]b(y)\,dy=0 \tag{33-a.1}$$

In this situation the solution is $y(r) = y_a(r) = l_0/r$ and the required condition about the range of values for curvature radii is:

$$h_2 \le y_2 = r-\frac{(1-e_s)l_0}{y'(r)} = e_s r \quad \Leftrightarrow \quad r \ge \frac{h_2}{e_s} = r_1 \tag{33-a.2}$$

(obviously the most extended cross section part with respect to the neutral axis is the one that has to be compared with radius dimension).

The required loading bending moment as a function of the radius r is:

$$M_a(r)=\int_{-h_1}^{h_2}E\left[\frac{(r-y)y_a'(r)}{l_0}-1\right]yb(y)\,dy=-\frac{E}{r}\int_{-h_1}^{h_2}y^2b(y)\,dy=-\frac{E}{3r}\left(h_2^3b_2+h_1^3b_1\right)$$

$$\Leftrightarrow \quad M_a(r)=-\frac{Eb_2h_2^3}{3r}\left(1+d^{-1}\right) \tag{33-a.3}$$

When $r = r_1$ we are able to calculate the bending moment that causes the first plasticization of the farther fibres with respect to the neutral axis:

$$M_{ip} = M_a(r_1) = -\frac{Eb_2h_2^2e_s}{3}\left(1+d^{-1}\right) \tag{33-a.4}$$

For the case (30-b), when the cross section is partially perfectly elastic and partially plastic, the equilibrium is given by:

$$\begin{aligned}0 &= \int_{-h_1}^{r-\frac{(1-e_s)l_0}{y_b(r)}}\left[\frac{(r-y)y_b(r)}{l_0}-1\right]b(y)\,dy - e_s\int_{r-\frac{(1-e_s)l_0}{y_b(r)}}^{h_2} b(y)\,dy \\ &= \frac{y_b(r)b_1h_1^2}{2l_0}+\frac{y_b(r)rb_1h_1}{l_0}-b_1h_1+\frac{b_2l_0}{2y_b(r)}-rb_2+\frac{y_b(r)r^2b_2}{2l_0}-\frac{b_2l_0e_s^2}{2y_b(r)}+rb_2e_s+ \\ &\quad -b_2h_2e_s-\frac{b_2l_0e_s}{y_b(r)}+\frac{b_2l_0e_s^2}{y_b(r)}\end{aligned}$$

Developing we have:

$$\left(r^2b_2+2rb_1h_1+b_2h_2^2\right)y_b^2-2\left[rb_2(1-e_s)+b_1h_1+b_2h_2e_s\right]l_0y_b+\left(b_2-2b_2e_s+b_2e_s^2\right)l_0^2=0$$

$$\Rightarrow\quad \left(r^2+2rdh_2+h_2^2\right)y_b^2-2\left[r(1-e_s)+dh_2+h_2e_s\right]l_0y_b+(1-e_s)^2l_0^2=0 \tag{33-b.1}$$

From which it is possible to calculate $y_b(r)$ by choosing the solution fitting $y_a(r)$ in $r = r_1$. In symbols:

$$y_b(r)=\frac{r(1-e_s)+h_2(d+e_s)+\sqrt{h_2(d+1)\left[2re_s(1-e_s)+h_2(d+2e_s-1)\right]}}{r^2+2rdh_2+h_2^2}l_0 \tag{33-b.2}$$

The verification of the continuity of $y(r)$ in the connection point r_1 is reported below:

$$y_a(r_1)=\frac{e_s}{h_2}l_0$$

$$y_b(r_1)=\frac{\frac{h_2(1-e_s)}{e_s}+h_2(d+e_s)+\sqrt{h_2(d+1)\left[2h_2(1-e_s)+h_2(d+2e_s-1)\right]}}{\left(\frac{h_2}{e_s}\right)^2+\frac{2d}{e_s}h_2^2+h_2^2}l_0=\frac{e_s}{h_2}l_0$$

The bending moment can be calculated as follows:

$$M_b(r) = Eb_1\int_{-h_1}^{0}\left[\frac{(r-y)y_b(r)}{l_0}-1\right]y\,dy + Eb_2\int_{0}^{r-\frac{(1-e_s)l_0}{y_b(r)}}\left[\frac{(r-y)y_b(r)}{l_0}-1\right]y\,dy + \\ -Ee_sb_2\int_{r-\frac{(1-e_s)l_0}{y_b(r)}}^{h_2} y\,dy$$

$$\Rightarrow M_b(r) = -\frac{Eb_2h_2^2}{6}\left\{\frac{y_b(r)h_2}{l_0}\left[-\left(\frac{r}{h_2}\right)^3+3\frac{r}{h_2}+2d^{-1}\right]+3(1-e_s)\left[\left(\frac{r}{h_2}\right)^2-1\right]\right\}+ \\ -\frac{Eb_2h_2^2}{6}(1-e_s)^2\left[-3\left(\frac{y_b(r)h_2}{l_0}\right)^{-1}\frac{r}{h_2}+\left(\frac{y_b(r)h_2}{l_0}\right)^{-2}(1-e_s)\right] \tag{33-b.3}$$

Before we move to case c, let us study the simpler case d, where the inner front y_2 crosses the centroid quote. Writing the equilibrium equation, we have:

$$0 = e_s\int_{-h_1}^{r-\frac{(1+e_s)l_0}{y_d(r)}} b(y)\,dy + \int_{r-\frac{(1+e_s)l_0}{y_d(r)}}^{r-\frac{(1-e_s)l_0}{y_d(r)}}\left[\frac{y_d(r)(r-y)}{l_0}-1\right]b(y)\,dy - e_s\int_{r-\frac{(1-e_s)l_0}{y_d(r)}}^{h_2} b(y)\,dy \\ = e_sb_1\left[r+h_1-\frac{(1+e_s)l_0}{y_d(r)}\right]+\frac{2e_sl_0b_1}{y_d(r)}\left(\frac{y_d(r)r}{l_0}-1\right)-\frac{b_1y_d(r)}{2l_0}\left(2r-\frac{2l_0}{y_d(r)}\right)\frac{2e_sl_0}{y_d(r)}+ \\ -e_sb_1\left[\frac{(1-e_s)l_0}{y_d(r)}-r\right]-e_sb_2h_2$$

Multiplying by $y_d(r)$ and dividing by e_s each term we obtain:

$$y_d(r)\left(2rb_1+b_1h_1-b_2h_2\right)-2b_1l_0=0$$

$$\Rightarrow y_d(r) = \frac{2b_1}{2rb_1+b_1h_1-b_2h_2}l_0 \tag{33-d.1}$$

The quote of the neutral axis is therefore:

$$y_n(r) = r-\frac{l_0}{y_d(r)} = -\frac{b_1h_1-b_2h_2}{2b_1} = -\frac{d-1}{2d^2}h_2 \tag{33-d.2}$$

It should be noted that, for these values of r, the neutral axis remains fixed in the position assumed as the cross section fully plasticizes.

The present configuration holds for negative y_2, so:

$$y_2 = re_s-\frac{1}{2b_1}(1-e_s)\left(b_1h_1-b_2h_2\right)\le 0$$

This permits to evaluate the superior endpoint r_3 of the radii interval:

$$r \le \frac{(1-e_s)(b_1h_1 - b_2h_2)}{2b_1e_s} = r_3 \tag{33-d.3}$$

The bending moment equation is:

$$M_d(r) = Ee_sb_1\int_{-h_1}^{r-\frac{(1+e_s)l_0}{y_d(r)}} y\,dy + Eb_1\int_{r-\frac{(1+e_s)l_0}{y_d(r)}}^{r-\frac{(1-e_s)l_0}{y_d(r)}}\left[\frac{(r-y)y_d(r)}{l_0} - 1\right]y\,dy +$$
$$-Ee_sb_1\int_{r-\frac{(1-e_s)l_0}{y_d(r)}}^{0} y\,dy - Ee_sb_2\int_0^{h_2} y\,dy$$

$$\Rightarrow M_d(r) = \frac{Eb_2e_sh_2^2}{12d^2}\left[3 - 6d - 9d^2 + e_s^2 - 2de_s^2 + \left(1 - \frac{4r}{h_2}\right)d^2e_s^2 + \frac{4r}{h_2}d^3e_s^2 + \left(\frac{2r}{h_2}\right)^2 d^4e_s^2\right] \tag{33-d.4}$$

Going back to case c, where the cross section begins to plasticize in the outer side, the corresponding equilibrium equation is:

$$0 = e_s\int_{-h_1}^{r-\frac{(1+e_s)l_0}{y_c(r)}} b(y)\,dy + \int_{r-\frac{(1+e_s)l_0}{y_c(r)}}^{r-\frac{(1-e_s)l_0}{y_c(r)}}\left[\frac{y_c(r)(r-y)}{l_0} - 1\right]b(y)\,dy - e_s\int_{r-\frac{(1-e_s)l_0}{y_c(r)}}^{h_2} b(y)\,dy$$
$$= e_sb_1\left[h_1 + r - \frac{(1+e_s)l_0}{y_c(r)}\right] + b_1\left[\frac{(1+e_s)l_0}{y_c(r)} - r\right]\left(\frac{y_c(r)r}{l_0} - 1\right) + \frac{b_1y_c(r)}{2l_0}\left[r - \frac{(1+e_s)l_0}{y_c(r)}\right]^2$$
$$-e_sb_2\left[h_2 - r + \frac{(1-e_s)l_0}{y_c(r)}\right] + b_2\left[r - \frac{(1-e_s)l_0}{y_c(r)}\right]\left(\frac{y_c(r)r}{l_0} - 1\right) - \frac{b_2y_c(r)}{2l_0}\left[r - \frac{(1-e_s)l_0}{y_c(r)}\right]^2$$

Multiplying each term by $y_c(r)$, we have:

$$0 = \frac{r^2}{2l_0}(b_1 - b_2)y_c(r)^2 - \left[r(b_1 - b_2) + re_s(b_1 + b_2) + b_1h_1e_s - b_2h_2e_s\right]y_c(r) + \frac{l_0}{2}(b_1 - b_2)$$
$$+l_0e_s(b_1 + b_2) + \frac{l_0e_s^2}{2}(b_1 - b_2) \tag{33-c.1}$$

Between the two solutions, the one that guarantees the continuity of $y(r)$ in r_3 is:

$$y_c(r) = \frac{rb_1 - rb_2 + rb_1e_s + rb_2e_s + b_1h_1e_s - b_2h_2e_s}{r^2(b_1 - b_2)}l_0 +$$
$$-\frac{l_0}{r^2(b_1 - b_2)}\left[-2rb_1b_2e_s(h_1 + h_2) + 2re_s\left(b_1^2h_1 + b_2^2h_2\right) + 2rb_1b_2e_s^2(h_1 - h_2) + \right. \tag{33-c.2}$$
$$\left. -2b_1b_2h_1h_2e_s^2 + 4r^2b_1b_2e_s^2 + 2re_s^2\left(b_1^2h_1 - b_2^2h_2\right) + \left(b_1^2h_1^2 + b_2^2h_2^2\right)e_s^2\right]^{\frac{1}{2}}$$

Indeed:

$$y_c(r_3)=\frac{r_3b_1-r_3b_2+r_3b_1e_s+r_3b_2e_s+b_1h_1e_s-b_2h_2e_s}{r_3^2(b_1-b_2)}l_0-\frac{b_1h_1-b_2h_2}{r_3^2(b_1-b_2)}l_0=\frac{2b_1e_s}{b_1h_1-b_2h_2}l_0$$
$$y_d(r_3)=\frac{2b_1l_0}{2r_3b_1+b_1h_1-b_2h_2}=\frac{2b_1l_0}{\frac{(1-e_s)(b_1h_1-b_2h_2)}{b_1e_s}b_1+b_1h_1-b_2h_2}=\frac{2b_1e_s}{b_1h_1-b_2h_2}l_0 \qquad \text{(33-c.3)}$$

When $r = r_2$ the plasticization of the outer section side is starting, namely $y_1 = -h_1$. Therefore, in order to determine r_2, the following system has to be solved:

$$\begin{cases} b_1\int_{-h_1}^{0}\left[\frac{(r_2-y)y_c(r_2)}{l_0}-1\right]dy+b_2\int_{0}^{r_2-\frac{(1-e_s)l_0}{y_c(r_2)}}\left[\frac{(r_2-y)y_c(r_2)}{l_0}-1\right]dy-e_sb_2\int_{r_2-\frac{(1-e_s)l_0}{y_c(r_2)}}^{h_2}dy=0 \\ r_2-\frac{(1+e_s)l_0}{y_c(r_2)}=-h_1 \end{cases}$$

$$\Leftrightarrow \begin{cases} b_1\left(\frac{y_c(r_2)r_2}{l_0}-1\right)h_1+\frac{b_1y_c(r_2)h_1^2}{2l_0}-e_sb_2\left[h_2-r_2+\frac{(1-e_s)l_0}{y_c(r_2)}\right] \\ \quad +b_2\left[r_2-\frac{(1-e_s)l_0}{y_c(r_2)}\right]\left(\frac{y_c(r_2)r_2}{l_0}-1\right)-\frac{b_2y_c(r_2)}{2l_0}\left[r_2-\frac{(1-e_s)l_0}{y_c(r_2)}\right]^2=0 \\ r_2=\frac{(1+e_s)l_0}{y_c(r_2)}-h_1 \end{cases} \qquad \text{(33-c.4)}$$

Substituting r_2 into the first equation we obtain:

$$y_c(r_2)^2\left(b_1h_1^2-b_2h_1^2\right)-y_c(r_2)\left(2b_1h_1l_0e_s-4b_2h_1l_0e_s-2b_2h_2l_0e_s\right)-4b_2l_0^2e_s^2=0$$

Between the two solutions, the one that guarantees the continuity of $y(r)$ in r_2 is:

$$y_c(r_2)=\frac{\left(b_1h_1-2b_2h_1-b_2h_2+\sqrt{-2b_1b_2h_1h_2+4b_2^2h_1h_2+b_1^2h_1^2+b_2^2h_2^2}\right)e_s}{(b_1-b_2)h_1^2}l_0$$
$$\Rightarrow r_2=\frac{2b_2h_1(1-e_s)+(1+e_s)\left(b_2h_2-b_1h_1+\sqrt{4b_2^2h_1h_2-2b_1b_2h_1h_2+b_1^2h_1^2+b_2^2h_2^2}\right)}{4e_sb_2} \qquad \text{(33-c.5)}$$

The bending moment equation becomes:

$$M_c(r)=Ee_sb_1\int_{-h_1}^{r-\frac{(1+e_s)l_0}{y_c(r)}}y\,dy+Eb_1\int_{r-\frac{(1+e_s)l_0}{y_c(r)}}^{0}\left[\frac{(r-y)y_c(r)}{l_0}-1\right]y\,dy+$$
$$+Eb_2\int_{0}^{r-\frac{(1-e_s)l_0}{y_c(r)}}\left[\frac{(r-y)y_c(r)}{l_0}-1\right]y\,dy-Ee_sb_2\int_{r-\frac{(1-e_s)l_0}{y_c(r)}}^{h_2}y\,dy$$

$$
\begin{aligned}
\Rightarrow M_c(r) = &-\frac{Eb_2h_2^2}{6}\left[\frac{y_c(r)h_2}{l_0}\left(\frac{r}{h_2}\right)^3(d-1)(d+1)\right]+\\
&-\frac{Eb_2h_2^2}{6}\left[\left(\frac{r}{h_2}\right)^2\left(3-3d^2-3d^2e_s-3e_s\right)+6e_s\right]+\\
&-\frac{Eb_2h_2^2}{6}\left[\left(\frac{y_c(r)h_2}{l_0}\right)^{-1}\frac{r}{h_2}\left(6e_s-3+3d^2-3e_s^2+6d^2e_s+3d^2e_s^2\right)\right]+\\
&-\frac{Eb_2h_2^2}{6}\left[\left(\frac{y_c(r)h_2}{l_0}\right)^{-2}\left(1-3e_s-d^2+3e_s^2-e_s^3-3d^2e_s-3d^2e_s^2-d^2e_s^3\right)\right]
\end{aligned}
\qquad (33\text{-c.6})
$$

A tedious but not difficult calculation shows that, when $h_2 \geq h_1$, the limiting radii satisfy the inequality $r_3 \leq r_2 \leq r_1$, as desired.

4. RESIDUAL CURVATURE EVALUATION

Once a certain loading bending moment $M(r)$ has been applied to the wire, a precise loading plasticization of the cross section is achieved. In order to evaluate the residual wire curvature we consider a linear unloading. With this assumption, the engineering strain formulation can be adopted to develop explicit calculation formulas. If we call r_{ul} the unloading radius with respect to the cross section centroidal axis and $y_{ul}(r_{ul})$ the unloading curvature angle depending on r_{ul}, the corresponding engineering strain will be:

$$
e_{ul}(r_{ul}, y) = \frac{(r_{ul}-y)y_{ul}(r_{ul})-l_0}{l_0} \qquad (34)
$$

The corresponding unloading normal stress is:

$$
s_{ul}(r_{ul}, y) = \begin{cases} Ee_{ul}(r_{ul}, y) + E\left(e_s - e(r, y)\right) & \text{if } y \leq y_1 \\ Ee_{ul}(r_{ul}, y) & \text{if } y_1 \leq y \leq y_2 \\ Ee_{ul}(r_{ul}, y) + E\left(-e_s - e(r, y)\right) & \text{if } y_2 \leq y \end{cases} \qquad (35)
$$

assuming, *a posteriori*, that this quantity satisfies the inequality $|s_{ul}(r_{ul})| < s_s$.

Imposing the equilibrium for the unloading phase over the cross section we have:

$$
\begin{aligned}
0 &= \int_{-\infty}^{\infty} s_{ul}(r_{ul}, y)\, b(y)\, dy \\
&= \int_{-\infty}^{+\infty} E e_{ul}(r_{ul}, y)\, b(y)\, dy + \int_{-\infty}^{y_1} E\big(e_s - e(r, y)\big) b(y)\, dy - \int_{y_2}^{+\infty} E\big(e_s + e(r, y)\big) b(y)\, dy \\
&= \frac{y_{ul}(r_{ul})\, r_{ul}}{l_0} A - A + \int_{-\infty}^{y_1} \big(e_s - e(r, y)\big) b(y)\, dy - \int_{y_2}^{+\infty} \big(e_s + e(r, y)\big) b(y)\, dy
\end{aligned}
\tag{36}
$$

Extracting $y_{ul}(r_{ul})$ from the previous equation we obtain:

$$
\frac{y_{ul}(r_{ul})}{l_0} = \frac{A - \int_{-\infty}^{y_1} \big(e_s - e(r, y)\big) b(y)\, dy + \int_{y_2}^{+\infty} \big(e_s + e(r, y)\big) b(y)\, dy}{A} \frac{1}{r_{ul}}
\tag{37}
$$

Observe that in the doubly symmetric case, this expression reduces to $1/r_{ul}$.

The unloading bending moment $M_{ul}(r_{ul})$ is given by:

$$
\begin{aligned}
M_{ul}(r_{ul}) &= \int_{-\infty}^{\infty} s_{ul}(r_{ul}, y)\, y b(y)\, dy \\
&= \int_{-\infty}^{+\infty} E e_{ul}(r_{res}, y)\, y b(y)\, dy + \int_{-\infty}^{y_1} E\big(e_s - e(r, y)\big) y b(y)\, dy + \\
&\quad - \int_{y_2}^{+\infty} E\big(e_s + e(r, y)\big) y b(y)\, dy \\
&= -E \frac{y_{ul}(r_{ul})}{l_0} J_C - E \int_{-\infty}^{y_1} e(r, y)\, y b(y)\, dy - E \int_{y_2}^{+\infty} e(r, y)\, y b(y)\, dy + \\
&\quad + E e_s \int_{-\infty}^{y_1} y b(y)\, dy - E e_s \int_{y_2}^{+\infty} y b(y)\, dy
\end{aligned}
\tag{38}
$$

Recalling equation (21) for the loading moment, we can observe that:

$$
M(r) - E \int_{y_1}^{y_2} e(r, y)\, y b(y)\, dy = E e_s \int_{-\infty}^{y_1} b(y)\, y\, dy - E e_s \int_{y_2}^{\infty} b(y)\, y\, dy
$$

Substituting into equation (38) we have:

$$
\begin{aligned}
M_{ul}(r_{ul}) &= -E \frac{y_{ul}(r_{ul})}{l_0} J_C - E \int_{-\infty}^{y_1} e(r, y)\, y b(y)\, dy - E \int_{y_2}^{+\infty} e(r, y)\, y b(y)\, dy + \\
&\quad + M(r) - E \int_{y_1}^{y_2} e(r, y)\, y b(y)\, dy \\
&= -E \frac{y_{ul}(r_{ul})}{l_0} J_C - E \int_{-\infty}^{\infty} \frac{(r - y) y'(r) - l_0}{l_0} y b(y)\, dy + M(r) \\
&= -E \frac{y_{ul}(r_{ul})}{l_0} J_C + E \frac{y'(r)}{l_0} J_C + M(r)
\end{aligned}
\tag{39}
$$

The residual radius r_{res} is given by the value of r_{ul} for which the above expression for $M_{ul}(r_{ul})$ equals zero:

$$\frac{y_{ul}(r_{res})}{l_0} = \frac{M(r)}{J_C E} + \frac{y(r)}{l_0} \tag{40}$$

Observe that in the doubly symmetric case, this equation reduces to the well-known formula:

$$\frac{1}{r_{res}} = \frac{M(r)}{J_C E} + \frac{1}{r}$$

Provided that the loading radius is known and is directly linked to the loading bending moment in each one of the four loading intervals previously characterized, the final wire curvature follows from the comparison between equations (37) and (40):

$$\frac{1}{r_{res}} \frac{A - \int_{-\infty}^{y_1} \left(e_s - e(r,y)\right) b(y)\, dy + \int_{y_2}^{+\infty} \left(e_s + e(r,y)\right) b(y)\, dy}{A} = \frac{M(r)}{J_C E} + \frac{y(r)}{l_0}$$

$$\Rightarrow \frac{1}{r_{res}} = \frac{A\left(\frac{M(r)}{J_C E} + \frac{y(r)}{l_0}\right)}{A - \int_{-\infty}^{y_1} \left(e_s - e(r,y)\right) b(y)\, dy - \int_{y_2}^{+\infty} \left(-e_s - e(r,y)\right) b(y)\, dy} = \frac{A\left(\frac{M(r)}{J_C E} + \frac{y(r)}{l_0}\right)}{A - I_1 - I_2} \tag{41}$$

For the chosen cross section the two integrals, I_1 and I_2, appearing at the denominator can be calculated for each of the four bending situations, *i.e.* (30-a), (30-b), (30-c) and (30-d), as follows.

If $r \geq r_1$,

$$I_1 = I_2 = 0 \tag{42-a}$$

If $r_2 \leq r \leq r_1$,

$$\begin{aligned} I_1 &= 0 \\ I_2 &= b_2 \int_{y_2}^{h_2} \left(-e_s - e(r,y)\right) dy \\ &= b_2 \left(-e_s - \frac{r y_b(r) - l_0}{l_0}\right) \int_{y_2}^{h_2} dy + b_2 \left(\frac{y_b(r)}{l_0}\right) \int_{y_2}^{h_2} y\, dy \\ &= b_2 \left(-e_s - \frac{r y_b(r) - l_0}{l_0}\right) (h_2 - y_2) + b_2 \frac{y_b(r)}{2 l_0} \left(h_2^2 - y_2^2\right) \end{aligned} \tag{42-b}$$

If $r_3 \leq r \leq r_2$,

$$
\begin{aligned}
I_1 &= b_1 \int_{-h_1}^{y_1} \left(e_s - e\left(r, y\right) \right) dy \\
&= b_1 \left(e_s - \frac{r y_c(r) - l_0}{l_0} \right) \int_{-h_1}^{y_1} dy + b_1 \left(\frac{y_c(r)}{l_0} \right) \int_{-h_1}^{y_1} y\, dy \\
&= b_1 \left(e_s - \frac{r y_c(r) - l_0}{l_0} \right) \left(y_1 + h_1 \right) + b_1 \frac{y_c(r)}{2 l_0} \left(y_1^2 - h_1^2 \right) \\
I_2 &= b_2 \left(-e_s - \frac{r y_c(r) - l_0}{l_0} \right) \left(h_2 - y_2 \right) + b_2 \frac{y_c(r)}{2 l_0} \left(h_2^2 - y_2^2 \right)
\end{aligned}
\tag{42-c}
$$

If $r \le r_3$,

$$
\begin{aligned}
I_1 &= b_1 \left(e_s - \frac{r y_d(r) - l_0}{l_0} \right) \left(y_1 + h_1 \right) + b_1 \frac{y_d(r)}{2 l_0} \left(y_1^2 - h_1^2 \right) \\
I_2 &= b_1 \int_{y_2}^{0} \left(-e_s - e\left(r, y\right) \right) dy + b_2 \int_{0}^{h_2} \left(-e_s - e\left(r, y\right) \right) dy \\
&= b_1 \int_{y_2}^{0} \left(-e_s - \frac{r y_d(r) - l_0}{l_0} \right) dy + b_1 \left(\frac{y_d(r)}{l_0} \right) \int_{y_2}^{0} y\, dy \\
&\quad + b_2 \int_{0}^{h_2} \left(-e_s - \frac{r y_d(r) - l_0}{l_0} \right) dy + b_2 \left(\frac{y_d(r)}{l_0} \right) \int_{0}^{h_2} y\, dy \\
&= -b_1 \left(-e_s - \frac{r y_d(r) - l_0}{l_0} \right) y_2 - b_1 \frac{y_d(r)}{2 l_0} y_2^2 \\
&\quad + b_2 \left(-e_s - \frac{r y_d(r) - l_0}{l_0} \right) h_2 + b_2 \frac{y_d(r)}{2 l_0} h_2^2
\end{aligned}
\tag{42-d}
$$

Therefore the provided set of equations enables to foresee with good accuracy the residual curvature of a wire characterized by the previously showed cross section.

Moreover, in order to guarantee the material integrity, it should be checked that the final plastic wire strain does not overcome a required limit. This typically corresponds to the rupture plastic strain of the wire material. To carry out that control it is necessary to consider the maximum final true wire strain over the cross section, namely:

$$
e_f(r,y)\Big|_{max} = \left\{ ln\left[\frac{y(r)(r-y)}{l_0} \right] \right\}\Bigg|_{max} \le e_r \tag{43}
$$

It should be noted that the initial bendable length does not influence any calculation. In fact it is a completely free parameter for a designer that applies the model since it is always coupled with the curvature angle terms.

5. A NUMERICAL EXAMPLE OF MODEL APPLICATION

A numerical example of model application is reported in the following. With reference to the cross section shape above illustrated (figure 2 and 3) we consider the following characteristic dimensions: b_1 = 3 mm, b_2 = 0.75 mm, h_1 = 1 mm and h_2 = 2 mm. The centroidal moment of inertia J_C equals 3 mm^4. It can be easily verified that $d = h_2/ h_1$ is greater than one and that condition (26) is satisfied.

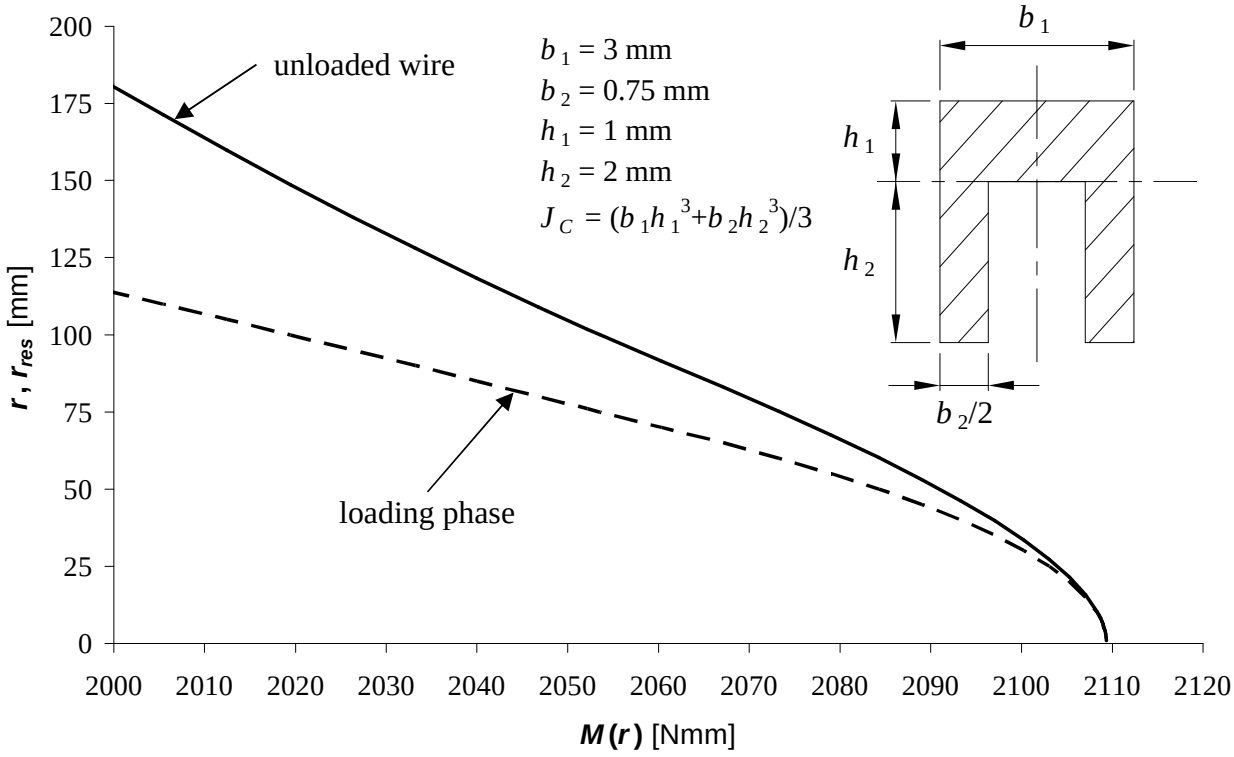

Figure 4: loading, unloading and residual radius of curvature with respect to the loading bending moment (elastic-perfectly plastic material behaviour; E = 206000 MPa, s_s = 750 MPa).

Considering an elastic-perfectly plastic material behaviour the required fundamental mechanical properties are Young's modulus *E*, equal to 206000 MPa as typically for steels, the yield strength s_s, 750 MPa, and the plastic true strain limit e_r, 0.3. The wire plasticization starts with a bending moment equal to 1125 Nmm (see equation (33-a.4)) and ends, with the cross section fully plasticized, when the moment, (see equation (29)), equals about 2109 Nmm.

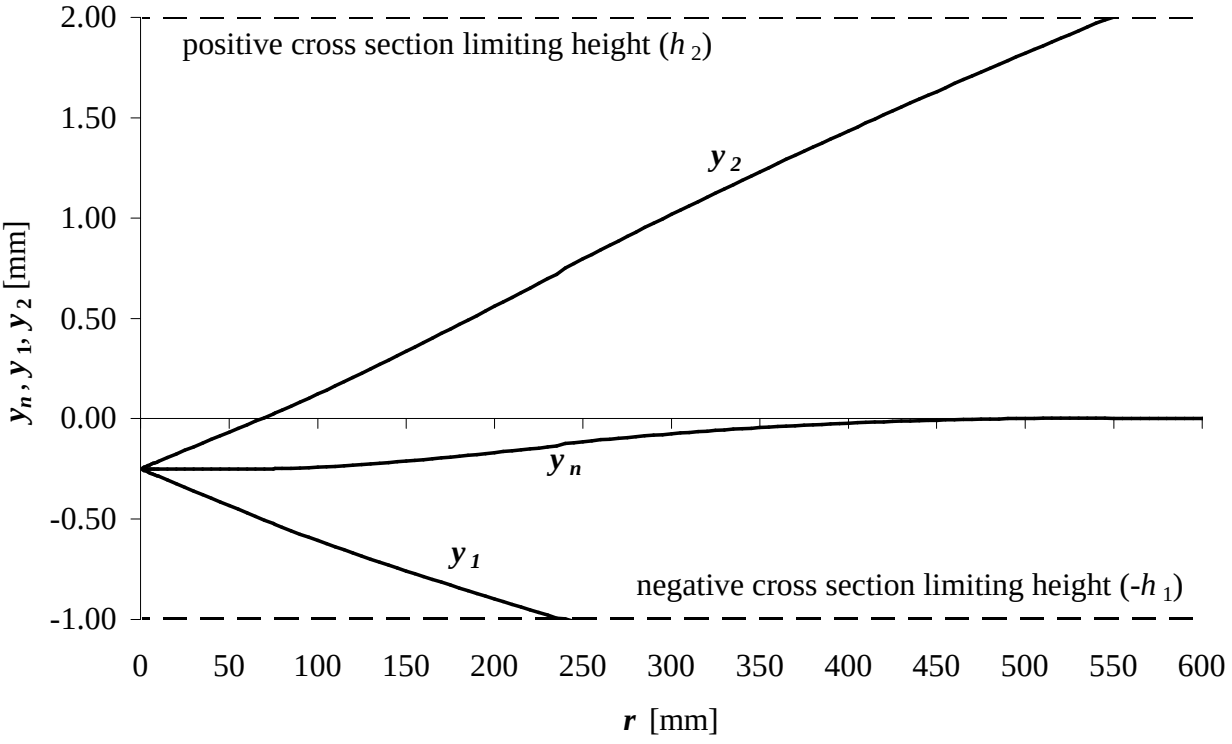

Figure 5: neutral axis and plasticization fronts displacements with respect to the loading radius of curvature.

In figure 4 the loading and the residual radius of curvature with respect to the applied loading bending moment are reported. The comparison between the two radii shows the entity of the springback for each applied moment. The values clearly converge when the loading bending moment has plasticized the whole cross section. Moreover, it is interesting to remark that for the considered material it is possible to bend the wire up to a 9 mm radius without exceeding the maximum true strain limit. Indeed by applying equation (43) it is possible to verify that for a loading radius of 9 mm we have a maximum true strain over the cross section of about 0.28 in modulus. Furthermore, the condition $|s_{ul}(r_{ul})| < s_s$ is satisfied: indeed $|s_{ul}(r_{ul})| < 656$ MPa for any value of the loading radius r.

Another interesting feature is the displacement of the neutral axis and the plasticization fronts during the loading phase. By means of the model it has been possible to plot their trend with the decreasing of the loading radius (figure 5). A neutral axis displacement can be observed after the plasticization of the first fibre at a distance of h_2 from it. This obviously happens on the more extended (along the y direction) cross section side and determines the negative direction of the neutral axis displacement. The convergence of the three displacement curves is asymptotic when the radius tends to zero. From figure 5 we can also see for which radius the negative cross section side

starts plasticizing (r_2, about 238 mm), particularly with respect to the other side (r_3, about 550 mm).

6. CONCLUSIONS

The analytical model developed and reported in this paper is focused on the relation between the nonlinear bending moment applied to a thin metallic wire and the corresponding residual radius of curvature. The set of analytical equations supplied by the model lets the designer choose the correct bending parameters, *i.e.* the bending moment, necessary to obtain the required final wire shape after the unloading springback. The nonlinearities due to the material behaviour that are taken into account are those of an elastic-perfectly plastic behaviour. The goal for the future is to continue the research by refining the model and developing more accurate material behaviours. The general form of the model has been developed and reported for a wire cross section nonsymmetric with respect to the centroidal axis, so as to show how the model could be applied to generic geometries. This lack of symmetry causes the displacement of the neutral axis. The calculations take this effect into account but at the same time they do not depend directly on it. The Bernoulli-Navier's hypothesis was adopted. Therefore the proposed model is applicable only if wire cross sections remain plane after bending rotations. This is very close to real material behaviour from the engineering point of view.

The proposed model allows predicting the final geometry of a wire after bending loading and unloading operations. The model enables to determine the stress and strain cross section state too. Considerations about fatigue behaviour and material damaging can consequently be formulated. The designer can introduce into the model the main mechanical characteristics of the wire material. The reported numerical example of model application allows to appreciate the large deformations, down to extremely small radii of curvature, and the neutral axis displacement during bending in the plastic range.

REFERENCES

[1] Icardi, U., "Large bending actuator made with SMA contractile wires", *Composites: Part B*, 32 (2001), 259-267.

[2] Verduzco, J.A., Hand, R.J. and Davies, H.A., "Fatigue behaviour of Fe-Cr-Si-B metallic glass wires", *International Journal of Fatigue*, 24 (2002), 1089-1094.

[3] Wagner, M., Sawaguchi, T., Kausträter, G., Höffken, D., Eggeler, G., "Structural fatigue of pseudoelastic NiTi shape memory wires", *Materials Science and Engineering A*, 378 (2004),

105-109.

[4] Shima, Y., Otsubo, K., Yoneyama, T., Soma, K., “Anisotropic orthodontic force from the hollow super-elastic Ti-Ni alloy wire cross-section”, *Journal of Materials Science: Materials in Medicine*, 13 (2002), 197-202.

[5] Lekston, Z., Drugacz, J., Morawiec, H., “Application of superelastic NiTi wires for mandibular distraction”, *Materials Science and Engineering*, A 378 (2004), 537–541.

[6] Wilkinson, P.D., Dysart, P.S., Hood, J.A.A., Herbison, G.P., “Load-deflection characteristics of superelastic nickel-titanium orthodontic wires”, *American Journal of Orthodontics and Dentofacial Orthopedics*, 121 (2002), 483-495.

[7] Ludwick, P., (1903) ‘Engineering Study of Sheet Bending’, Verlag des Deutschen Polytechnischen Vereins, Böhmen, *Technische Blätter*, Vol. 35, pp. 133-159.

[8] Lubhan, J. and Sachs, G., “Bending of an ideal plastic metal”, *Trans. ASME*, 72 (1950), 201-208.

[9] Hill, R., “The Mathematical Theory of Plasticity”, Clarendon, Oxford, 1950.

[10] Wang, C., Kinzel, G. and Altan, T., “Mathematical Modeling of Plane-Strain Bending of Sheet and Plate”, *Journal of Materials Processing Technology*, 39 (1993), 279-304.

[11] Wang, J.F., Wagoner, R.H., Matlock, D.K., Barlat, F., “Anticlastic curvature in draw-bend springback”, *International Journal of Solids and Structures*, 42 (2005), 1287-1307.

[12] Datsko, J. and Yang, C. T., “Correlation of Bendability of Materials With Their Tensile Properties”, *ASME Journal of Engineering for Industry* (1960), 309-314.

[13] Stachowicz, F. “Experimental and numerical study of springback problems in sheet metal bending”, *Archives of metallurgy*, 48 (2) (2003), 161-172.

[14] Ling, Y.E., Lee, H.P., Cheok, B.T., “Finite element analysis of springback in L-bending of sheet metal”, *Journal of Materials Processing Technology*, 168 (2005), 296–302.

[15] Esat, V., Darendeliler, H., Gokler, M.I., “Finite element analysis of springback in bending of aluminium sheets”, *Materials and Design*, 23 (2002), 223-229.

[16] Papeleux, L., Ponthot, J.P., “Finite element simulation of springback in sheet metal forming”, *Journal of Materials Processing Technology*, 125–126 (2002), 785–791.

[17] Alves, J.L., Oliveira, M.C., Menezes, L.F., “Springback evaluation with several phenomenological yield criteria”, *Advanced Materials Forum II Materials Science Forum*, 455-456 (2004), 732-736.

[18] Math, M., Grizelj, B., “Finite element approach in the plate bending process”, *Journal of Materials Processing Technology*, 125-126 (2002), 778-784.

[19] Chan, W.M., Chew, H.I., Lee, H.P., Cheok, B.T., “Finite element analysis of spring-back of

V-bending sheet metal forming processes", *Journal of Materials Processing Technology*, 148 (2004), 15–24.

[20] Chun, B.K., Jinn, J.T., Lee, J.K., "Modeling the Bauschinger effect for sheet metals, part I: theory", *International Journal of Plasticity*, 18 (2002), 571–595.

[21] Chun, B.K., Jinn, J.T., Lee, J.K., "Modeling the Bauschinger effect for sheet metals, part II: applications", *International Journal of Plasticity*, 18 (2002), 597–616.

[22] Gau, J.T., Kinzel, G.L., "A new model for springback prediction for aluminium sheet forming", *Journal of Engineering Materials and Technology – Transactions of the ASME*, 127 (3) (2005), 279-288.

[23] Gan, W., Wagoner, R.H., "Die design method for sheet springback", *International Journal of Mechanical Sciences*, 46 (2004), 1097-1113.

[24] Mullan, H.B., "Improved prediction of springback on final formed components", *Journal of Materials Processing Technology*, 153-154 (2004), 464-471.

[25] Hino, R., Goto, Y., Yoshida, F., "Springback of sheet metal laminates in draw-bending", *Journal of Materials Processing Technology*, 139 (2003), 341-347.

[26] Kruger, J.B., Palazotto, A.N., "An Investigation of Springback in Wire Products", *ASME Journal of Engineering for Industry* (1972), 329-335.

[27] Palazzotto, A.N., Seccombe Jr., D.A., "Springback of Wire Products Considering Natural Strain", *ASME Journal of Engineering for Industry* (1973), 809-814.

[28] Paolini, G., "Il comportamento dei fili di acciaiosotto sforzi di flessione, con particolare riferimento al campo delle medie deformazioni", *Ingegneria Meccanica* (1960), 10-11-12.

[29] Khromov, I.V., "Computer modeling of the processes of elastoplastic deformation of a wire in the course of winding", *Strength of Materials*, 35 (6) (2003), 638-642.

[30] Goes, B., Gil-Sevillano, J. and D'Haene, U., "Modelling the evolution of residual stresses during tensile testing of elastoplatic wires subjected to a previous bending operation", *International Journal of Mechanical Sciences*, 41 (1999), 1031-1050.

[31] Luis, C.J., León, J. and Luri, R., "Comparison between finite element method and analytical methods for studying wire drawing processes", *Journal of Materials Processing Technology*, 164-165 (2005), 1218-1225.

[32] Chen, S.H., Wang, T.C., "A new hardening law for strain gradient plasticity", *Acta mater.*, 48 (2000), 3997-4005.

[33] Richard Liew, J.Y., Thevendran, V., Shanmugam, N.E., Tan, L.O., "Behaviour and Design of Horizontally Curved Steel Beams", *J. Construct. Steel Research*, 32 (1995), 37-67.

[34] Dadras, P., "Plane strain elastic-plastic bending of a strain-hardening curved beam",

International Journal of Mechanical Sciences, 43 (2001), 39-56.

[35] Koursunsky, A.M. and Withers, P.J., 'Plastic bending of residually stressed beam', *Int. J. Solids Structures*, 34(16) (1997), 1985-2002.

[36] Sokolinsky, V.S., Shen, H., Vaikhanski, L. and Nutt S.R., "Experimental and analytical study of nonlinear bending response of sandwich beams", *Composite Structures*, 60 (2003), 219-229.

[37] Baragetti, S., "A Theoretical Study on Nonlinear Bending of Wires", *Meccanica*, 41 (4) (2006) 443-458.

[38] Belluzzi, O., "Scienza delle costruzioni" Vol. 1, 2, 3, 4, Zanichelli, Bologna,1995.

[39] Bertram, A., "Elasticity and plasticity of large deformations: an introduction", Springer, Berlin (etc.), 2005.

[40] Kachanov, L.M., "Fundamentals of the theory of plasticity", Dover, Mineola (Ney York), 2004.

[41] Lubarda, V.A., "Elastoplasticity theory", CRC press, Boca Raton (etc.), 2002.

[42] Khan, A.S., Huang, S., "Continuum theory of plasticity", Wiley, New York, 1995.

[43] Lubliner, J., "Plasticity theory", Macmillan, New York, 1990.

[44] Honeycombe, R.W.K., "The plastic deformation of metals" Arnold, London, 1968.

NOMENCLATURE

A	wire cross section area
$b(y)$	wire cross section width
C	cross section centroid
E	Young's modulus of wire material
h_1	maximum cross section outer distance from centroid
h_2	maximum cross section inner distance from centroid
J_C	cross section moment of inertia about the centroidal axis
l_0	starting wire bendable length
$l(r, y)$	actual wire bent length with respect to a generic cross section quote
$M(r)$	loading bending moment applied to the wire for a certain loading radius
M_{ip}	initial plasticization bending moment
M_{fp}	full plasticization bending moment
$M_{ul}(r_{ul})$	unloading bending moment applied to the wire for a certain unloading radius
r	actual radius of curvature due to the bending load with respect to the centroidal axis
r_{res}	residual radius of curvature after the unloading with respect to the centroidal axis

r_{ul}	unloading radius of curvature with respect to the centroidal axis
y	generic fibre vertical quote with respect to centroid
y_n	neutral axis vertical quote with respect to centroid
$y_1(r)$	vertical first yielding quote in the wire outer side
$y_2(r)$	vertical first yielding quote in the wire inner side
$e(r, y)$	cross section strain for a certain radius of curvature
$e_e(r, y)$	engineering strain for a certain radius of curvature
$e_f(r, y)$	actual strain corresponding to the final wire configuration
e_r	actual strain corresponding to the material rupture
e_s	engineering strain corresponding to the material yield stress
$e_{ul}(r_{ul}, y)$	engineering unloading strain for a certain unloading radius of curvature
$s\ (r, y)$	normal stress over the wire cross section
s_s	material yield stress
$y(r)$	actual curvature angle spanned by the actual bent wire length
$y_{ul}(r_{ul})$	unloading curvature angle spanned by the actual bent wire length